

Synthesis and characterization of X8R BaTiO₃-based dielectric ceramics by doping with NiNb₂O₆ nanopowders

Lingxia Li¹ · Jingyang Yu¹ · Ning Zhang¹ · Jing Ye¹

Received: 15 June 2015 / Accepted: 8 October 2015 / Published online: 12 October 2015
© Springer Science+Business Media New York 2015

Abstract High performance X8R BaTiO₃-based ceramics with pure perovskite phase were prepared by nanocomposite doping method. The phase structure, dielectric and electrical properties and the “relaxorlike” characteristic of ceramic materials are systemically studied. According to XRD and TEM analysis, the nanocomposite dopants via sol–gel method are uniform and well dispersive. The role of NiNb₂O₆ on dielectric properties and phase structure of BaTiO₃-based ceramics is investigated. The properties comparison of samples prepared by nano-doping and conventional process is accomplished. SEM micrographs reveal that the grain size of BaTiO₃-based samples is more uniform by nano-doping process. Meanwhile, bulk densities and dielectric properties are enhanced. The 1.5 wt% NiNb₂O₆-doped sample sintered at 1280 °C shows the optimal dielectric performance ($\epsilon_r = 4160$, $\tan\delta < 1.0\%$, $\Delta C/C_{20\text{ °C}} \leq \pm 15\%$) that satisfied EIA–X8R specification.

1 Introduction

The material systems with higher Curie temperatures are desirable for MLCC applications at harsh working conditions, e.g. aerospace, oil exploration and in civil fields. For instance, the working temperature of an electronic control unit placed in an automotive engine may be higher than

130 °C. Therefore, X8R ceramics (-55 to 150 °C, $\Delta C/C_{20\text{ °C}} \leq \pm 15\%$), whose properties are defined by the Electronic Industries Alliance (EIA), are of increasing importance in the rapidly growing electronics industry [1, 2].

The development tendency of multi-layer ceramic capacitors (MLCCs) is high-capacitance small size, which requires the dielectric materials achieving higher permittivity with a uniform grain size [3]. As a ferroelectric perovskite ceramic, BaTiO₃ (BT) exhibits high permittivity at room temperature. It is not only widely used as a conventional ferroelectric but also recently introduced in components of MLCCs [3, 4]. However, the sharply change in dielectric constant at Curie temperature of BaTiO₃ has limited its application due to a relatively narrow using temperature range. Thus, BaTiO₃ is chemically modified to meet the required dielectric temperature characteristic by doping with depressors. There are a series of co-doping systems for achieving a good dielectric property, such as BaTiO₃–Yb₂O₃–MgO [5], BaTiO₃–Nb₂O₅–Co₃O₄ [6], and BaTiO₃–Nb₂O₅–Ni₂O₃ [7], which only meet the X7R specifications (-55 to 125 °C, $\Delta C/C \leq 15\%$). Several BaTiO₃-based X8R ceramics have been reported, such as BaTiO₃–Y₂O₃–MgO–SiO₂ [8], BaTiO₃–Y₂O₃–MgO–Mn₃O₄–SiO₂–CaO [9], which have low dielectric constant ($\epsilon_r < 3000$). In this study, CaZrO₃ is chosen as the dopants to obtain a flat TCC curve, which shifts the Curie point to higher temperature [10], to replace Pb-based ceramics for environmental protection and human health [11].

BaTiO₃-based ceramics result from the formation of a “core-shell” structure, with the core being a pure BaTiO₃ phase and the shell of BaTiO₃ with other oxide dopants [5–9]. As the core-shell structure is unstable in thermodynamics, the key issue for the formation of the core-shell structure is not only the selection of proper additives that react with BaTiO₃ grains. The other important factor is the

✉ Lingxia Li
llx66_tju@163.com

¹ Key Laboratory for Advanced Ceramics and Machining Technology of Ministry of Education and School of Electronic and Information Engineering, Tianjin University, Tianjin 300072, China

uniform distribution of the dopants around the BaTiO₃ particles, especially when BaTiO₃ grains become smaller. For the conventional solid-state method, large particles of the additives may induce local segregation of the additives in the dielectric layers and cause an initial loss of the insulation resistance of MLCCs. A new nanocomposite doping process has been developed by researchers [8, 12, 13], which can be effective in controlling the particle size of additives and enhance the mixed homogeneity of minor constituents. In this study, the effects of nano-NiNb₂O₆ in improving dielectric properties of the BaTiO₃-based ceramics has been researched.

2 Experimental procedure

2.1 Sample preparation

The NiNb₂O₆ nanopowders were synthesized by the sol-gel process. Analytically pure (AR) Ni(NO₃)₂·6H₂O and Nb₂O₅ were used as the raw materials. Citric acid and ethylene glycol were used as a chelating agent and reaction medium. The experimental procedure for preparing the NiNb₂O₆ nanopowders was shown in Fig. 1. Niobium and nickel compounds were also prepared by solid-state method (NiNb₂O₆ synthesized from NiO and Nb₂O₅ with average particle size of 0.4 and 0.5 μm). The CaZrO₃ was obtained after calcining the mixture of CaCO₃ and ZrO₂ at 1000 °C for 2 h by conventional solid-state method. The base material was BaTiO₃ powder (Guoci Co. Ltd., China). BaTiO₃ and all the additives were weighed and mixed with deionized water by ball milling (using ZrO₂

beads) for 4 h and then dried. After drying, mixed powders were added in 7.0 wt% binder wax, and then pressed into disks with 15 mm in diameter and 1 mm in thickness. The disks were sintered at 1280 °C for 3 h in air, using a heating rate of 5 °C/min. Silver was applied on both sides of the as-fired samples to obtain the electrodes of capacitors. The sample added with 0.5–2.0 wt% NiNb₂O₆ nanopowders were named as A05 ~ A20 respectively. The sample B15 was prepared by adding 1.5 wt% NiNb₂O₆ which was obtained by conventional process.

2.2 Characterization

Phase identification and lattice parameters were characterized by X-ray diffraction (XRD) patterns, which were obtained from D/MAX-B Model X-ray diffractometer (D8-Focus; Bruker AXS GmbH, Karlsruhe, German) with CuKα radiation at 40 kV and 40 mA. Microstructural properties such as grain size distribution and morphology were examined using a transmission electron microscopy (TEM, JEM-2100F, JEOL, Ltd., Tokyo, Japan) and a field-emission scanning electron microscopy (FE-SEM, S-4800; Hitachi, Ltd., Tokyo, Japan). The bulk density of the samples was measured by the Archimedes method. Dielectric loss and the capacitance were measured by the use of capacitance meter (HP4278A; Hewlett-Packard, Santa Clara, CA) at 1 kHz from –55 to 150 °C. The temperature was controlled by GZ-ESPEC oven. Insulation resistivity was measured using a high resistance meter (Agilent 4339B, Santa Clara, CA) at room temperature. The frequency characteristics were measured between 50 Hz and 100 kHz, using a TH2828S automatic component analyzer.

3 Results and discussion

3.1 Characterization of nano-dopants

The gels are calcined in air at 600 and 800 °C for 2 h respectively, and their XRD patterns are illustrated in Fig. 2. The XRD indicates the presence of Ni₂O₃ (JCPDS 14-481) and Nb₂O₅ (JCPDS 19-862) at 600 °C, NiNb₂O₆ (JCPDS: 31-906) with phase pure is clearly found at 800 °C. The crystal structure of NiNb₂O₆ is orthorhombic and all the d-lines match with reported values [14]. The sharp diffraction peaks appear distinctly for the NiNb₂O₆ calcined at 800 °C. This indicates that NiNb₂O₆ changed from amorphous to crystalline phase with increase of calcining temperature [15]. TEM is used to further examine the particle size, crystallinity and morphology of samples. Figure 3 shows the TEM bright field images of the NiNb₂O₆ calcined 600 and 800 °C. Figure 3a indicates that agglomeration of particles is serious when NiNb₂O₆

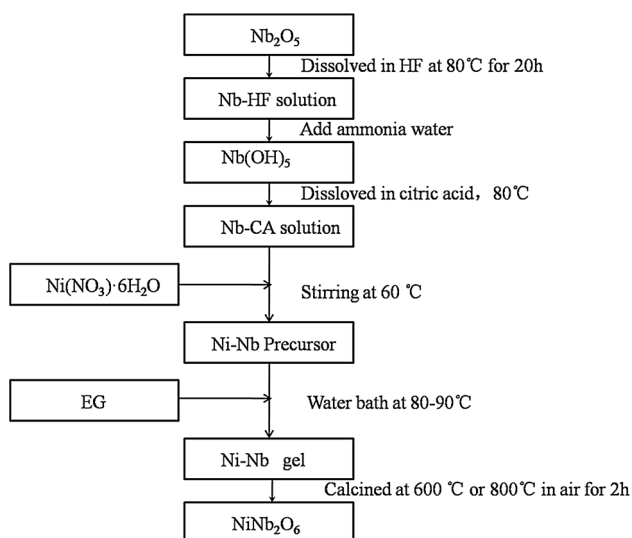


Fig. 1 Flow chart for preparing the NiNb₂O₆ nanopowders by the sol-gel process

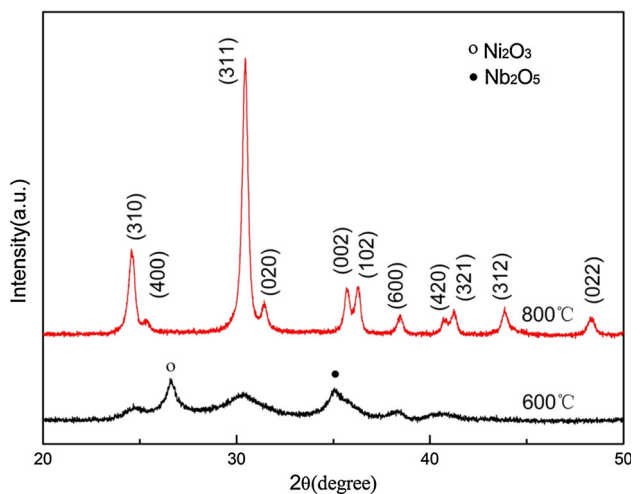
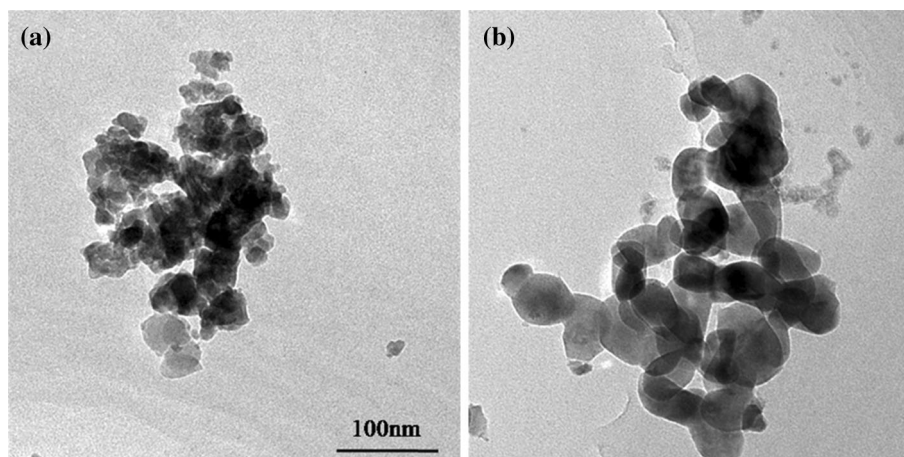


Fig. 2 XRD patterns of NiNb_2O_6 nanopowders sintered at 600 and 800 °C

Fig. 3 TEM photos of NiNb_2O_6 nanopowders sintered at **a** 600, **b** 800 °C



calcined at 600 °C. Meanwhile, it can be estimated that the particle size of sample in Fig. 3b is nanoscale (an average particle size of 63.9 nm) with better dispersion. Hence, a relative higher calcining temperature of 800 °C need be adopted to achieve well dispersive and crystalline nanoparticles.

3.2 Dielectric properties and phase structure of samples by doping NiNb_2O_6 nanopowders

Figure 4 presents the temperature dependence of the dielectric constant ϵ_r of the sample A05 ~ A20 at measuring at 1 kHz. Two dielectric constant peaks are observed in the dielectric constant-temperature curves (ϵ_r -T curves). The dielectric peak at about 130 °C is certainly associated with the paraelectric to ferroelectric transition of the grain core, whereas the peak at lower temperature is due to strong chemical inhomogeneity of grain shell [16, 17].

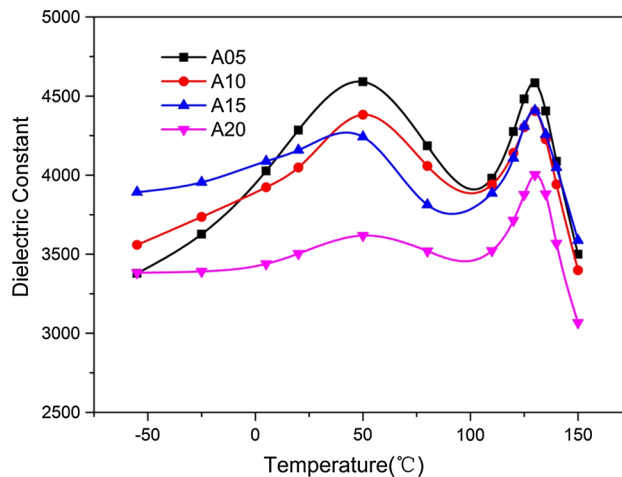


Fig. 4 Temperature dependence of dielectric constant for samples with various amounts of NiNb_2O_6 nanopowders sintered at 1280 °C

Ni^{2+} , Nb^{5+} cations are easier to diffuse into the crystal lattice by using the $\text{NiO-Nb}_2\text{O}_5$ composite oxide as dopants, which is attributed to the identity of $(\text{Ni}_{1/3}^{2+}\text{Nb}_{2/3}^{5+})^{4+}$ and Ti^{4+} (The effective radius of Ti^{4+} is 0.061 and $(\text{Ni}_{1/3}^{2+}\text{Nb}_{2/3}^{5+})^{4+}$ is 0.066 nm in the sixfold coordination [16]) as we reported previously [18]. Furthermore, the valence of the complex $(\text{Ni}_{1/3}^{2+}\text{Nb}_{2/3}^{5+})^{4+}$ is identical to Ti^{4+} . It is effective to inhibit the generation of oxygen vacancies which are introduced to compensate for the charge deficiency of Ni ions on Ti sites [19], as shown in Eq. (1).



A certain amount of $(\text{Ni}_{1/3}^{2+}\text{Nb}_{2/3}^{5+})^{4+}$ ions substituting for Ti^{4+} ions forms the chemically inhomogeneous structure and the compositional inhomogeneity might induce diffuse phase transition characteristics, which results in a multi-peaks character over a relatively wide temperature range.

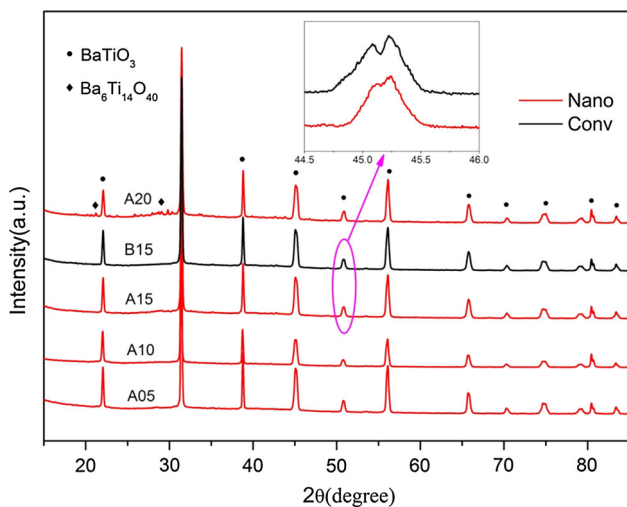


Fig. 5 XRD patterns of samples with various amounts of NiNb₂O₆ sintered at 1280 °C

Figure 5 shows the XRD patterns of various amounts of NiNb₂O₆-doped BT-based ceramics sintering at 1280 °C. When the doping amount of NiNb₂O₆ is < 2.0 wt%, the XRD results demonstrate that all the samples display a desired perovskite structure, which indicates that the NiNb₂O₆ have diffused into the BaTiO₃ lattice to form a solid solution. The dielectric constant decreases significantly when 2.0 wt% NiNb₂O₆ nano-dopants is added to BaTiO₃ as shown in Fig. 4. Because (Ni²⁺_{1/3}Nb⁵⁺_{2/3})⁴⁺ composite cation would easily diffuse into the crystal lattice and replace the Ti⁴⁺ cation, and the redundant Ti⁴⁺ cation reacts with the BaTiO₃ and forms a Ba₆Ti₁₇O₄₀ (JCPDF 77-1566) second phase (low dielectric constant ~ 59) [20]. In summary, the optimal dielectric properties are achieved when 1.5 wt% NiNb₂O₆ nano-dopants is added.

3.3 Properties analysis of samples prepared by nano-doping and conventional process

Figure 5 also shows the XRD patterns of the sample A15 and B15. It can be seen that two samples display a desired perovskite structure, which indicates there is no secondary

phase in existence for both cases. As we know, the tetragonal structure is characterized by (200) and (002) peak splitting around 45° and the pseudo-cubic structure is characterized by (200) peak around 45° [11, 21, 22]. The diffraction peaks around 45° are separated from each other, which indicate that the crystal structure of sample B15 is typically tetragonal [23]. The two diffraction peaks merge into one peak, confirming that the tetragonality (c/a ratio) of sample A15 decreased as shown in Table 1. The grain shell is considered to be non-ferroelectric phase, which results in the decrease of ferroelectric percentage (tetragonality) [22]. The tetragonality decreases, which suggests that the volume fraction of the tetragonal grain core decreases, whereas the volume fraction of the cubic grain shell increases for samples prepared by nano-doping method.

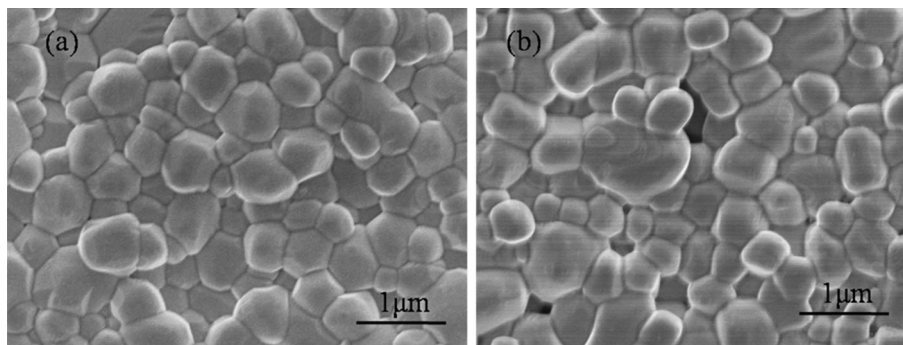
Figure 6 shows FE-SEM images of sample A15 and B15, and no second phase is observed in both samples. Coarse grains (~ 1.0 μm) together with fine grains (~ 0.5 μm) are detected for sample B15, resulting in the distribution of the grain sizes is uneven. Furthermore, the pores and voids in existence lead to the relatively low density (~ 5.76 g/cm³). On the contrary, sample A15 exhibits a very dense, uniform and fine-grained microstructure with smooth surface and clear boundaries. The sintered density is about 5.89 g/cm³ using Archimedes’ method and the average grain size is < 0.6 μm by the linear interception method. This illustrates that the nano-dopants could inhibit the grain growth more efficiently and be helpful to form the dense and homogeneous fine-grained ceramics.

As shown in Fig. 7a, the dielectric constant exhibits a broadened and diffuse ferroelectric-paraelectric phase transition for both samples. It is supposed that the substitution of Ti sites by (Ni²⁺_{1/3}Nb⁵⁺_{2/3})⁴⁺ in the shell regions of BaTiO₃ grains is responsible for this behavior. The dielectric constant at room temperature is enhanced to 4160 (A15) via nano-doping, which satisfies EIA–X8R specification as shown in Fig. 7b. The increasing of ε_{20°C} can attribute to the increasing grain size of fine-grained BT ceramics [21]. The Curie temperature (T_c) of the sample

Table 1 Lattice parameters of and electrical properties of NiNb₂O₆-doped BaTiO₃ samples in room temperature

Sample	NiNb ₂ O ₃ content (wt%)	c/a	Eb (kV/mm)	ρ _v (10 ¹² Ω cm)	ε _r	tgδ (%)	T _c (°C)	ΔC/C _{20 °C} (%)		
								–55 °C	125 °C	150 °C
A05	0.5	1.0042	9.87	8.89	4284	1.067	128.2	–21.1	4.6	–18.3
A10	1.0	1.0027	10.21	10.95	4048	0.943	128.5	–12.1	6.3	–16.1
A15	1.5	1.0012	13.77	13.98	4160	0.854	128.7	–6.4	3.6	–13.7
B15	1.5	1.0036	10.09	8.92	4055	1.116	127.8	–12.3	18.1	–18.5
A20	2.0	1.0010	10.36	6.77	3503	1.097	128.7	–3.4	10.6	–12.4

Fig. 6 SEM photos of samples with 1.5 wt% NiNb₂O₆ prepared by **a** nano-doping and **b** conventional process sintered at 1280 °C



B15 is about 127.8 °C, Meanwhile, the T_c of sample A15 rise to about 128.7 °C. The Curie temperature increases, which can also be explained by internal tensile stress model the internal stresses are also responsible for the permittivity increase [10, 12]. We deem that NiNb₂O₆ is mainly located in grain shells, and the internal stress induced by the lattice mismatch between cores and shells. The tensile stress stabilizes the tetragonal phase and shifts T_c to a higher point. In comparison with B15, the dielectric constant peak of A15 at T_c is markedly depressed. The peak intensity is associated with the volume fraction of the grain core [8]. Table 1 shows the dielectric properties of the sample A15 and B15. Insulation resistance of the sample B15 is lower than 10¹³ Ω cm. However, resistance significantly increases via nano-doping and sample A15 shows resistance larger than 10¹³ Ω cm. Owing to lower porosity, dielectric loss of the sample A15 decreases to 0.854 %. These intriguing properties of sample prepared by nano-doping process make this material get qualified for practical applications. Table 2 shows the dielectric properties of some X8R materials which were prepared by nanocomposite doping method. Doping NiNb₂O₆ nanopowders is more effective to improve the dielectric constant at room temperature.

The variations of relative permittivity of NiNb₂O₆-doped ceramic samples at various frequencies (50 Hz–100 kHz) are shown in Fig. 8. A diffuse transition with frequency dispersion above and around the permittivity peak in the room temperature was observed. The permittivity of the both samples decrease obviously with the increasing frequency in the low-temperature (–55 ~ 110 °C), but no significant differences are observed in high-temperature (110–150 °C) [24, 25]. The variation width of the permittivity of sample B15 is slightly smaller than sample A15. Due to the particular characteristics of nanopowder, such as surface effect and small-scale effect (large specific surface area, high interfacial energy, and so on), the nano-doping ions behave a so strong tendency to be incorporated into BaTiO₃ lattice, the diffusion length of nano-dopants is deeper than that of submicron dopant. The average thickness of grain shell in the ceramic

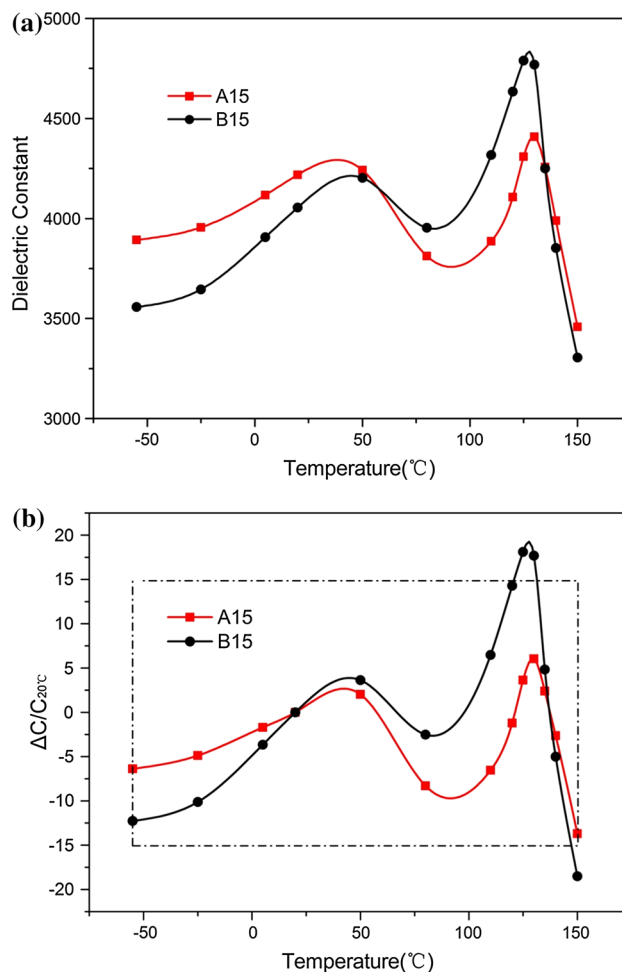


Fig. 7 Temperature dependence of **a** dielectric constant and **b** capacitance change for sample A15 and B15 sintered at 1280 °C

prepared by nano-doping is larger than that of conventional doping. The “relaxorlike” characteristic can be attributed to the oxygen vacancies, which is certificated by Ciomaga et al. [26] The experiment results proves the “core-shell” structure in another way: Curves in low-temperature represent non-ferroelectric phase (the shell) produced by ion doping, which affected by frequency significantly. On the contrary, curves in high-temperature mainly affected by

Table 2 Comparison of dielectric properties of some X8R materials which were prepared by nanocomposite doping method

Nos.	Material	S.T (°C)	ϵ_r	$\text{tg}\delta$ (%)	References
1	BaTiO ₃ + 1.5 wt% NiNb ₂ O ₆ (N.) + 2.0 wt% CaZrO ₃	1280	4160	0.8	This work
2	BaTiO ₃ + 2.0 wt% (Y–Mg–Si–O)(N.)	1260	2900	0.6	[8]
3	BaTiO ₃ + 3.0 wt% K _{0.5} Na _{0.5} NbO ₃ + 0.7 wt% (Li–Ti–Si–O)(N.)	1280	3960	0.8	[13]

S.T sintering temperature, N. nanopowders

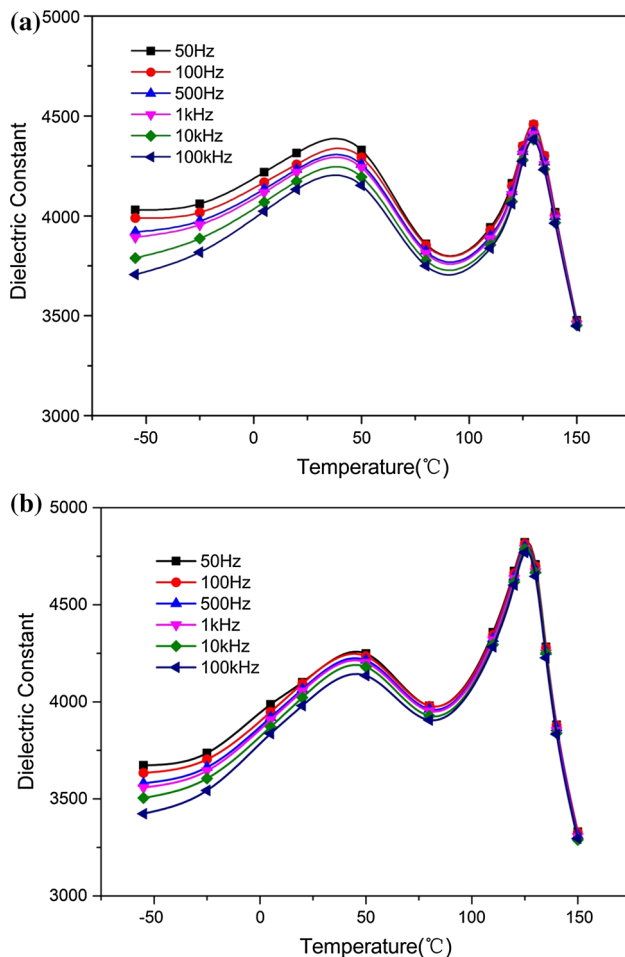


Fig. 8 Frequency dependence of dielectric constant for samples doped by 1.5 wt% NiNb₂O₆ prepared by **a** nano-doping and **b** conventional process sintered at 1280 °C

pure BT, which is ferroelectric phase (the core), have little difference with frequency [27]. So “relaxorlike” characteristic is enhanced with the increase of ratio of the grain shell due to the nano-doping process.

4 Conclusions

High performance BaTiO₃-based ceramics with different amounts of NiNb₂O₆ (0.5, 1.0, 1.5, 2.0 wt%) were synthesized by nanocomposite doping method and well

sintered at 1280 °C. XRD indicated the nanocomposite changed from amorphous to crystalline phase with increase of calcining temperature. TEM showed the nano-dopants acquired by sol–gel method are uniform and well dispersive, with an average particle size of 63.9 nm calcined at 800 °C. It showed great effects in improving properties of the BaTiO₃ ceramics by doping NiNb₂O₆ of nanopowders. Due to the uniform nanopowders as well as uniformly distributing in BaTiO₃ matrix and coating the BaTiO₃ particles completely, nano-dopants could inhibit grain growth efficiently and be favorable to form desired core-shell microstructure in the fine-grained BaTiO₃ ceramics. Besides, the new method played a crucial role to the stability of high-temperature dielectric properties, which shift the T_c to a higher temperature. The “relaxorlike” characteristic attributed to the increase of ratio of the grain shell due to the nano-doping. As a result, the 1.5 wt% NiNb₂O₆-doped sample exhibits the optimal dielectric properties with high dielectric constant $\epsilon_{20\text{ °C}} = 4160$, low dielectric loss $\text{tan}\delta < 1.0\%$, and flat TCC curve $\Delta C/C_{20\text{ °C}} \leq \pm 14\%$, -55 to 150 °C , which satisfies EIA–X8R specification.

References

- D.H. Choi, A. Baker, M. Lanagan, S. Trolier-Mckinstry, C. Randall, Structural and dielectric properties in (1–x)BaTiO₃–xBi(Mg_{1/2}Ti_{1/2})O₃ ceramics (0.1 ≤ x ≤ 0.5) and potential for high-voltage multilayer capacitors. *J. Am. Ceram. Soc.* **96**, 2197–2202 (2013)
- L.X. Li, D. Guo, W.S. Xia, Q.W. Liao, Y.M. Han, Y. Peng, An ultra-broad working temperature dielectric material of BaTiO₃-based ceramics with Nd₂O₃ addition. *J. Am. Ceram. Soc.* **95**, 2107–2109 (2012)
- Z.B. Shen, X.H. Wang, H.L. Gong, L.W. Li, L.T. Li, Effect of MnO₂ on the electrical and dielectric properties of Y-doped Ba_{0.95}Ca_{0.05}Ti_{0.85}Zr_{0.15}O₃ ceramics in reducing atmosphere. *Ceram. Int.* **40**, 13833–13839 (2014)
- Y.L. Li, Z.L. Liao, F. Fang, X.H. Wang, L.T. Li, J. Zhu, Significant increase of Curie temperature in nano-scale BaTiO₃. *Appl. Phys. Lett.* **105**, 182901 (2014)
- N. Kikuchi, T. Ogasawara, S. Iwaya, Development of dielectric material with X8R characteristic. *Ceram. Trans.* **32**, 191–200 (1993)
- H. Chazono, H. Kishi, Sintering characteristics in BaTiO₃–Nb₂O₅–Co₃O₄ ternary system. *J. Am. Ceram. Soc.* **82**, 2689–2697 (1999)

7. S. Wang, S.R. Zhang, X.H. Zhou, B. Li, Z. Chen, Investigation on dielectric properties of BaTiO₃ co-doped with Ni and Nb. *Mater. Lett.* **60**, 909–911 (2006)
8. B. Li, S.R. Zhang, X.H. Zhou, S. Wang, Z. Chen, Preparation of BaTiO₃-based ceramics by nanocomposite doping process. *J. Mater. Sci.* **42**, 2090–2096 (2007)
9. Z.B. Tian, X.H. Wang, H. Gong, T.H. Song, K.H. Hur, L. Li, Core-shell structure in nanocrystalline modified BaTiO₃ dielectric ceramics prepared by different sintering methods. *J. Am. Ceram. Soc.* **94**, 973–977 (2011)
10. G.F. Yao, X.H. Wang, T.Y. Sun, L.T. Li, Effects of CaZrO₃ on X8R nonreducible BaTiO₃-based dielectric ceramics. *J. Am. Ceram. Soc.* **94**, 3856–3862 (2011)
11. V.V. Shvartsman, D.C. Lupascu, Lead-free relaxor ferroelectrics. *J. Am. Ceram. Soc.* **95**, 1–26 (2012)
12. X.H. Zhou, S.R. Zhang, Y. Yuan, B. Li, J.S. Liu, Preparation of BaTiO₃-based nonreducible X7R dielectric materials via nanometer powders doping. *J. Mater. Sci.: Mater. Electron.* **17**, 133–136 (2006)
13. Z.Y. Hu, B. Cui, M. Li, L.L. Li, Novel X8R-type BaTiO₃-based ceramics with a high dielectric constant created by doping nanocomposites with Li-Ti-Si-O[J]. *J. Mater. Sci.: Mater. Electron.* **24**, 3850–3855 (2013)
14. V. Samuel, A.B. Gaikwad, A.D. Jadhav, N. Natarajan, V. Ravi, A coprecipitation technique to prepare NiNb₂O₆ [J]. *Mater. Lett.* **61**, 2354–2355 (2007)
15. Y.Y. Zhou, M.K. Lü, Z.F. Qiu, A.Y. Zhang, Q. Ma, H.P. Zhang, Z.S. Yang, Photoluminescence of NiNb₂O₆ nanoparticles prepared by combustion method. *Mater. Sci. Eng., B* **140**, 128–131 (2007)
16. C.R. Zhou, X.Y. Liu, Effect of B-site substitution by (Ni_{1/3}Nb_{2/3})⁴⁺ for Ti⁴⁺ on microstructure and piezoelectric properties in (Bi_{1/2}Na_{1/2})TiO₃ piezoelectric ceramics. *J. Alloys Compd.* **466**, 563–567 (2008)
17. M. Kahn, Influence of grain growth on dielectric properties of Nb-doped BaTiO₃. *J. Am. Ceram. Soc.* **54**, 455–457 (1971)
18. L.X. Li, R.X. Fu, Q.W. Liao, L.J. Ji, Doping behaviors of NiO and Nb₂O₅ in BaTiO₃ and dielectric properties of BaTiO₃-based X7R ceramics. *Ceram. Int.* **38**, 1915–1920 (2012)
19. Y. Sun, H.X. Liu, H. Hao, Z. Song, S.J. Zhang, Structure property relationship in BaTiO₃-Na_{0.5}Bi_{0.5}TiO₃-Nb₂O₅-NiO X8R system. *J. Am. Ceram. Soc.* **98**, 1574–1579 (2015)
20. X. Xu, G.E. Hilmas, Effects of Ba₆Ti₁₇O₄₀ on the dielectric properties of Nb-doped BaTiO₃ ceramics. *J. Am. Ceram. Soc.* **89**, 2496–2501 (2006)
21. S.J. Kuang, X.G. Tang, L.Y. Li, Y.P. Jiang, Q.X. Liu, Influence of Zr dopant on the dielectric properties and Curie temperatures of Ba(Zr_xTi_{1-x})O₃ (0 ≤ x ≤ 0.12) ceramics. *Scripta Mater.* **61**, 68–71 (2009)
22. M. Ganguly, S.K. Rout, T.P. Sinha, S.K. Sharma, H.Y. Park, I.W. Kim, Characterization and Rietveld refinement of A-site deficient lanthanum doped barium titanate. *J. Alloy. Compd.* **579**, 473–484 (2013)
23. P. Gao, Y.P. Pu, P. Li, T. Wu, Effects of BaNb₂O₆ addition on microstructure and dielectric properties of BaTiO₃ ceramics. *J. Mater. Sci.: Mater. Electron.* **24**, 3958–3962 (2013)
24. F. Boujelben, H. Khemakhem, A. Simon, Effect of Mn and Nb Doped BaTiO₃ in the dielectric properties in the Ba (Mn_{1/2}Nb_{1/2})_xTi_{1-x}O₃. *J. Electron. Mater.* **41**, 2250–2255 (2012)
25. L.W. Wu, X.H. Wang, H.L. Gong, Y.A. Hao, Z.B. Shen, L.T. Li, Core-satellite BaTiO₃@ SrTiO₃ assemblies for a local compositionally graded relaxor ferroelectric capacitor with enhanced energy storage density and high energy efficiency. *J. Mater. Chem. C* **3**, 750–758 (2015)
26. C.E. Ciomaga, M.T. Buscaglia, V. Buscaglia, L. Mitoseriu, Oxygen deficiency and grain boundary-related giant relaxation in Ba(Zr, Ti)O₃ ceramics. *J. Appl. Phys.* **110**, 114110 (2011)
27. H.L. Cheng, H.L. Du, W.C. Zhou, D.M. Zhu, F. Luo, B.X. Xu, Bi (Zn_{2/3}Nb_{1/3}) O₃-(K_{0.5}Na_{0.5}) NbO₃ high-temperature lead-free ferroelectric ceramics with low capacitance variation in a broad temperature usage range. *J. Am. Ceram. Soc.* **96**, 833–837 (2013)